Biomedical Microdevices (2019) 21: 19
https://doi.org/10.1007/s10544-019-0365-1

Microfabricaton of microfluidic check valves using comb-shaped moving plug for suppression of backflow in microchannel

Jini Hyeon[1,2] · Hongyun So[1,2]

Published online: 21 February 2019

Abstract
This study reports on an efficient microscale one-way valve system that combines the physical properties of photopolymerized microstructures and viscoelastic microchannels to rectify flows with low Reynolds numbers. The comb-shaped moving plug in the microchannel prevented backflow in the closed state to ensure that the microchannel remained completely blocked in the closed state, but allowed forward flow in the open state. This microfluidic check valve was microfabricated using the combination of the soft lithography and the releasing methods with the use of a double photoresist layer to create microchannels and free-moving comb-shaped microstructures, respectively. As a result, the microfluidic check valves elicited average high-pressure differences as much as 10.75 kPa between the backward and forward flows at low Reynolds numbers of the order of 0.253, thus demonstrating efficient rectification of microfluids. This study supports the use of rectification systems for the development of biomedical devices, such as drug delivery, micropumps, and lab-on-a-chip, by allowing unidirectional flow.

Keywords Microfluidic check valve · Comb-shaped structures · Moving plug · Biomedical devices · Low Reynolds number

1 Introduction

Control of fluids at the microscale is a core issue for various applications of biomedical microdevices. The advent of microfluidic circuit components similar to autonomous electronic components, such as resistors, diodes, and capacitors, could significantly impact chemical (deMello 2006; Irimia et al. 2006) and biological applications (Lagally et al. 2001; Wang et al. 2004). In many applications, a check, or alternatively a one-way valve—the most fundamental fluid control element—plays an important role in microfluidic systems, such as in drug delivery systems where backflow must be prevented. Such one-way 'microfluidic check valve' used in microfluidics, is analogous to an electronic diode, thereby preventing fluid flow in a certain direction, and thus serving as a rectifier.

Various types of one-way valves have extensively been investigated for a wide variety of applications, including chemical reaction, chromatography, and biomedical systems (Gravesen et al. 1993; Oh and Ahn 2006). Most of them can be achieved by several fabrication processes using an element of cantilevers (Xu et al. 2001; Zengerle et al. 1995) and designed membranes (Bien et al. 2003; Chung et al. 2003; Hu et al. 2004; Nguyen et al. 2004; Nguyen and Truong 2004; Zhang et al. 2016; Zhang et al. 2015). Such microfluidic systems enable operation in a range of *Reynolds number* (*Re*) between 0.01 and 1000 (Gravesen et al. 1993). In particular, many lab-on-a-chip (LOC) and biomedical microdevices applications, such as point-of-care, onsite chemical detection, and molecular diagnostics, rely on flow resistance under a low *Re*, in which the resistance in a microchannel is virtually invariant for both forward and backward flow directions (i.e., isotropic), regardless of the channel shape (Groisman and Quake 2004). Clearly, special designs of passive microfluidic valves are required for low-*Re* flows which are inevitable in LOC, whose flow resistance must be controllable (i.e., anisotropic) for practical applications in the field of microfluidics.

The introduction of a multilayer elastomeric fluidic valve, known as a *Quake valve*, provided the foundation of the first generation of integrated microfluidic circuits (Hong et al. 2004; Lee et al. 2005; Thorsen et al. 2002; Unger et al. 2000). Such Quake valve-based systems, however, require expensive external pneumatic pressure control equipment for

✉ Hongyun So
hyso@hanyang.ac.kr

[1] Department of Mechanical Engineering, Hanyang University, Seoul 04763, South Korea

[2] Institute of Nano Science and Technology, Hanyang University, Seoul 04763, South Korea

device operation. Although self-regulating microfluidic check valves, which do not require external control, have been investigated to overcome this issue, most of them were primarily constructed by means of multilayer fabrication processes at an increased cost in terms of fabrication, time, and labor (Lamont et al. 2017; Leslie et al. 2009; Mosadegh et al. 2010; Weaver et al. 2010). In the case of the flap-type check valves, which could be fabricated using simple procedures, they did not work properly in regions with *Re* values less than 0.5 (Adams et al. 2005; Loverich et al. 2007). Consequently, research has shifted toward the development of self-regulating, inexpensive, simple, and efficient microfluidic check valves. For example, previous studies have demonstrated microfluidic check valves that utilized suspended microbeads to rectify flow in conditions associated with low-*Re* values, which were less than unity (Ou et al. 2012; Sochol et al. 2014). Unfortunately, these microbead-based systems had issues pertaining to the loading, handling, and clogging of microbeads in the microchannel (Henry et al. 2012; Kim and Kim 2014; Massenburg et al. 2016; Sochol et al. 2012a, b; Wyss et al. 2006). To prevent the clogging issue, several microfluidic systems have recently been developed using various platforms (Cheng et al. 2016; Huang et al. 2014).

The fabrication of free-moving elements within fluidic systems by optofluidic lithography has emerged as a potential technique for constructing components of micro/nanofluidic circuits. Previously, researchers have employed the optofluidic lithography method to fabricate free-moving microscale pistons and one-way valves in microfluidic systems (Hasselbrink et al. 2002; Kirby et al. 2005; Kirby et al. 2002; Reichmuth et al. 2004). The movements of these components, however, were limited owing to the high pressures required for device operation. Even though several self-regulating microfluidic check valves have been implemented using optofluidic lithography (Beebe et al. 2000; Kim and Beebe 2007; Sochol et al. 2013a, b; Vázquez and Paull 2010), device functionality required changes in the properties of the working fluid, such as pH and temperature. Accordingly, these systems have also suffered from leakage issues due to the clearance between the microchannel and blocking microstructures during reverse flow. Therefore, the development of functional microfluidic check valves for operation in applications associated with low-*Re* flows using simple, robust, faster, inexpensive, and more reliable operations, still remains a significant practical engineering challenge. In this study, we demonstrate a reliable microfluidic check valve based on a comb-shaped moving plug (CMP) using double-layered photoresist photolithography to fabricate a free-moving comb-shaped (or finger-shaped) microstructure, which is capable of flow rectification under low-*Re* conditions with a near-perfect on/off valve system. The chronic leakage issue in reverse flow can be dramatically improved by the multiple blocking of flows based on the use of the CMP, as shown in Fig. 1.

2 Theoretical design

For most applications, the effectiveness of the microfluidic check valves is related to the difference of the flow resistance in the reverse flow direction (closed-valve state) and that of the opposite flow direction (open-valve state). This quantity can be expressed mathematically as the difference between the reverse pressure drop and the forward pressure drop across the valve under a fixed flow rate (Q), as follows

$$\Delta P_{valve} = \left(\Delta P_{reverse} - \Delta P_{forward}\right)_Q. \quad (1)$$

In general, a high value of ΔP_{valve} is desirable in many LOC applications because it generates efficient flow rectification. To obtain a high ΔP_{valve} values for low-*Re* flows, the fluid leakage passing through valve microstructures during reverse flow should be minimized to ensure a large pressure difference across the valve. Fig. 1 shows a schematic of the microcheck valve system using the CMP developed in this study. Since most microchannels are made of polydimethylsiloxane (PDMS) with viscoelastic properties, it contributes to the leakage of the fluid during the device's operation owing to the potential deformation of PDMS as the flow rate increases

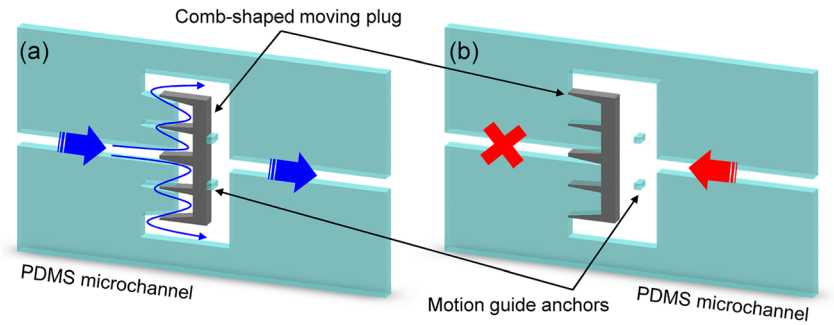

Fig. 1 Conceptual illustration of the microfluidic check valve based on comb-shaped moving plug: **a** open state: the comb-shaped microstructure is released from the entrance of the microchannel to allow fluid flow, **b** closed state: the microstructure is interlocked with microchannels which obstruct fluid flow

(Sochol et al. 2013a, b). Therefore, one of the key requirements for achieving an improved ΔP_{valve} performance is the capability to prevent leakage flows with a unique valve system. In reverse flow, the microcheck valve with the CMP was designed to suppress the deformation of PDMS by interlocking the PDMS microchannel with comb-fingers, as shown in Fig. 1b. For forward flow, the comb-shape microstructure moves along the flow direction from the closed to the open position due to hydrodynamic forces. The motion of the comb-shaped microstructure is guided by a pair of anchors (motion guide anchors). When the flow direction is reversed, the comb-shaped microstructure returns to the closed position, thereby blocking all reverse flows through the interlocked fingers. Since fluids must pass through the surface of each finger of the comb-shaped microstructure (i.e., obstacles from the viewpoint of fluids), the flow resistance during reverse flow was dramatically increased owing to the increased contact area with the fluids. This also implies that the device performance highly depends on the number of CMP fingers. Consequently, in this study, microcheck valves with various numbers of fingers (i.e., single-, triple-, and quintuple-finger microstructures) were fabricated and characterized to investigate the effect of the number of fingers on ΔP_{valve}.

To estimate the hydraulic characteristics of the microcheck valve with pressure and velocity fields across the CMP finger structure, three-dimensional finite element analysis was performed using ANSYS (Workbench 13.0), as shown in Fig. 2. For the simulation, quintuple-finger microstructure was used as a reference case. Continuous fluid and isothermal models were used to observe the pressure field when the comb-shaped microstructure is open and interlocked with the PDMS microchannel. Figure 2a and c show the contour of the pressure field across the system under *Re* of approximately 0.2 for forward and reverse flow, respectively. As a result of simulation, the pressure drop across the valve during the reverse flow was much larger than the pressure drop during the forward flow, demonstrating the prevention of backflow in the closed state. Figure 2b and d present the streamline fields across the valve system under forward and reverse flow, respectively. As shown in figure, the CMP in the microchannel prevented backflow in the closed state due to the multiple blocking by the finger structures, while it normally passes through surrounding the microstructure under forward flow (see Fig. 2b).

3 Experimental methods

The overall fabrication process included two main processes: standard soft lithography and photolithography for generating microfluidic channels and for creating the CMP, respectively. The schematic of the overall fabrication process for the microcheck valve using the CMP is illustrated in Fig. 3. The microchannels were fabricated using a standard soft lithography step with PDMS. The negative photoresist, SU-8 2100 (MicroChem Corp.), was first spin-coated on a separate, clean, 4 in. silicon wafer, at 1900 rpm for 30 s, followed by photolithography (MIDAS, MDA-400M) with 19 mW/cm^2 for 12 s, and subsequent development in SU-8 developer for 20 min. The prepared silicone elastomer, PDMS (Sylgard 184, Dow Corning, NY), at a 10:1 (base:curing agent) ratio was then poured onto the developed SU-8 patterned wafer (Fig. 3b). After curing at 120 °C for 2 h, the PDMS microchannels were separated from the wafer and individual channels were cut through a razor blade. The biopsy punches were used to create ports at the inlet and outlet locations. To fabricate the suspended moving microstructures, photolithography using a double photoresist layer was employed in this study. This method has been reported previously to release

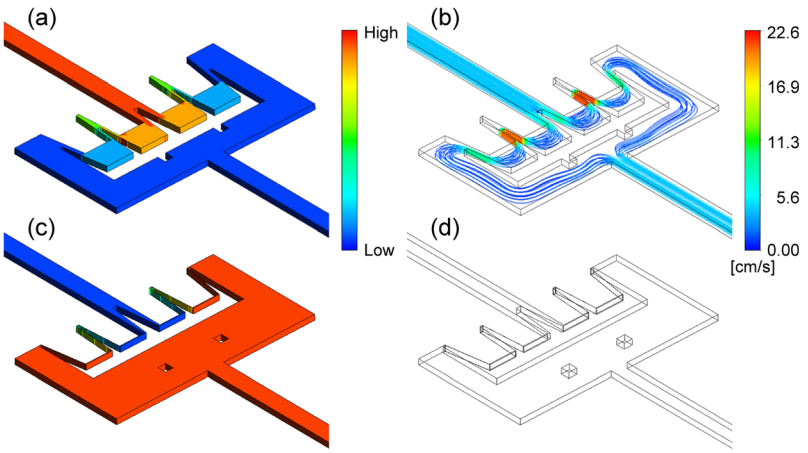

Fig. 2 Three-dimensional ANSYS simulation results under an approximate *Re* of 0.2: **a** pressure field and **b** streamline for the open state, **c** pressure field and **d** streamline for the closed state

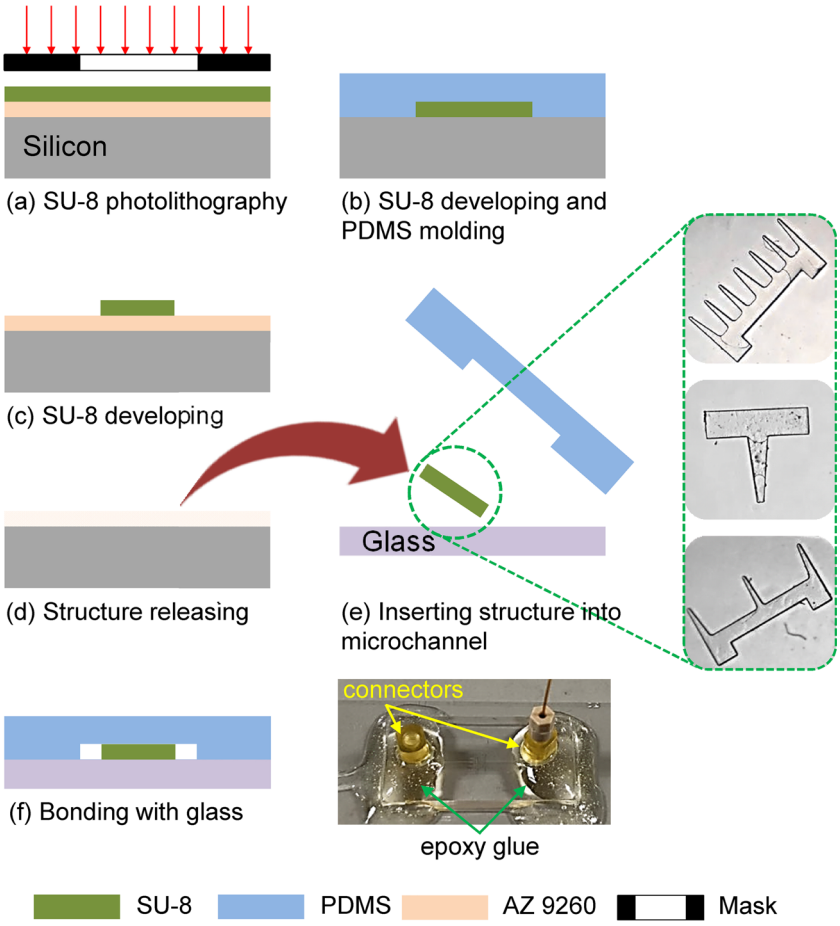

Fig. 3 Schematic of overall fabrication processes of the microfluidic check valve using a comb-shaped moving plug: **a** standard photolithography on the silicon wafer coated with double-layered photoresists (SU-8 2100 and AZ 9260 to create moving microstructures and sacrificial layer, respectively), **b** standard soft lithography to fabricate PDMS microchannels, **c** development of patterned comb-shaped microstructures in the SU-8 developer, **d** release process of microstructures by dissolving AZ 9260 (sacrificial layer) in the SU-8 developer, **e** integration of suspended comb-shaped microstructures into microchannels on the glass, and **f** final bonding between PDMS microchannel and glass

SU-8 structures from the substrate (Lau et al. 2013). As a first step, positive photoresist (AZ 9260, MicroChemicals GmbH) was spin-coated onto a clean 4 in. silicon wafer at 1500 rpm for 80 s, thus serving as a sacrificial layer with an approximate thickness of 19 μm. The SU-8 2100 was then spin-coated again onto a positive photoresist-deposited wafer at 3100 rpm for 30 s. After depositing the double-layered photoresists film, the micropatterns of the CMP were defined using photolithography with 19 mW/cm^2 applied for 48 s (Fig. 3a). The excessive UV exposure time increased the degree of cross-linking of the photoresist, preventing potential flexure or deterioration of SU-8 microstructures during the development process. The exposed wafer was then developed in the SU-8 developer for 10 min (Fig. 3c), and comb-shaped microstructures made of SU-8 were finally released in the developer by dissolving the positive photoresist underneath the SU-8 negative photoresist (Fig. 3d). The released comb-shaped microstructure was placed on a microscope glass slide (Fisher Scientific Co., LLC), and the fabricated PDMS microchannel was aligned (Fig. 3e) and bonded with the glass (Fig. 3f). Finally, connectors were glued to the inlet and outlet locations with epoxy at a 1:1 (resin:hardener) ratio to prevent leakage of the fluid at the inlet and outlet. To characterize the fabricated microstructures and microchannels, a scanning electron microscope (SEM, S-4800, Hitachi Ltd.) and a surface profiler (Alpha-Step 500, KLA-Tencor) were used to measure the height of both microstructures and microchannels. To demonstrate the rectifying performance of the fabricated microcheck valve, the actual movements of the suspended comb-shaped moving structures in low-*Re* flows were monitored using an EM-CCD (Electron Multiplying Charge-Coupled Device) camera (ImagEM X2, Hamamatsu Photonics K.K.). For the measurement of the pressure drop across the microcheck valve, a syringe pump (PHD ULTRA, Harvard Apparatus Ltd.) and a pressure sensor (40PC500G2A, Honeywell International Inc.) were used during the experiments.

4 Results and discussion

Figure 4a shows the fabricated PDMS microchannel where low-*Re* flows can be rectified by the comb-shaped microstructures. To investigate the effect of the number of fingers in the CMP, three different comb-shaped microstructures were fabricated in this study to have one, three, and five fingers, respectively. Figure 4b, c and d show the SEM images of CMPs with one (single), three (triple), and five (quintuple) fingers, respectively.

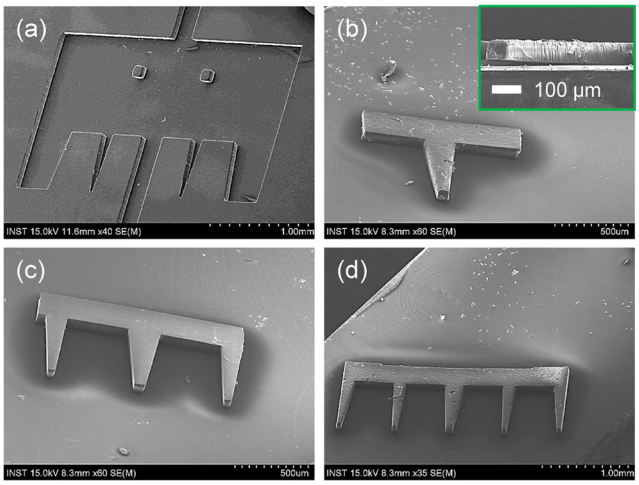

Fig. 4 SEM images at a tilted view of **a** the PDMS microchannel where low-*Re* flows can be rectified by the movement of the comb-shaped microstructures, and comb-shaped moving microstructure with **b** one (single) finger, **c** three (triple) fingers, and **d** five (quintuple) fingers

The height of microstructures was approximately 80 μm (see the inset of Fig. 4b), which was intentionally fabricated to have a value slightly smaller than the height of the PDMS microchannel (~95 μm). This small gap in the height between the microchannel and microstructure allows the CMP to move smoothly and prevents it from being stuck in the microchannel, which can be caused by upward bending (flexure) or the rough surfaces of the fingers during the release process in the aqueous SU-8 developer. Although this height difference might also cause a flow leakage in the closed state, it is significantly smaller compared to the overall amount of flow, and thus negligible. Figure 5 demonstrates the rectifying operation of microcheck valves with different number of fingers in the microchannel, captured from the EM-CCD camera during operation. In the microcheck valve with the CMP using the single finger, the microstructure moves up to the motion guide anchors under forward flow owing to hydrodynamic forces, as shown in Fig. 5a and b. The main role of the motion guide anchors was to guide translational motion and prevent unwanted rotational motion of the CMP such that the plug can be engaged smoothly with the entrance of the PDMS microchannel. The location of the motion guide anchors can also affect to the device performance, but ANSYS simulation revealed that the contribution of the motion guide anchors' position is relatively smaller than other parameters such as the number of fingers, a gap in the height between the microchannel and microstructure, and the flow rate. After the flow direction was reversed, the CMP moved back to the stationary comb-shaped PDMS wall. The shape of PDMS microchannel was designed to have similar shape of the CMP, such that CMP can be interlocked smoothly with the microchannel. Although dead volumes exist at side corners of the microchannel where bubbles are clogged, size of dead volumes gradually decreased as the flow rate increased. To minimize the bubble

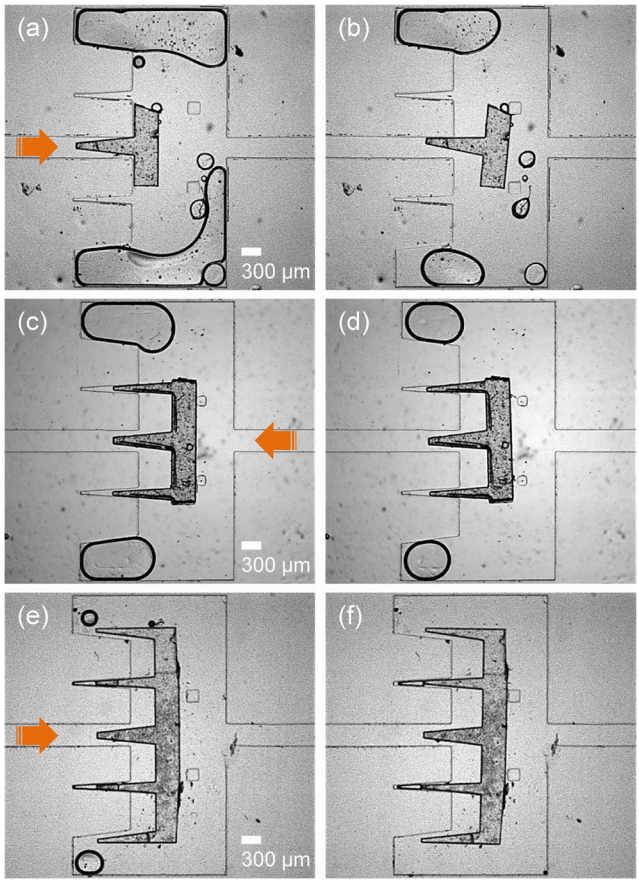

Fig. 5 Optical images of translational motion of comb-shaped moving microstructures with **a**,**b** single-, **c**,**d** triple-, and **e**,**f** quintuple-finger microstructures in response to changes in the flow direction: **a** forward flow (open state, 50 μl/min), **c** backward flow (closed state, 75 μl/min), and **e** forward flow (open state, 80 μl/min). Silicone oil with the viscosity of 30×10^{-6} m^2/s was used for experiments

clogging in the dead volumes, parametric studies for a design of microchannel will need to be considered. Figure 5c and d show the state change from the open to the closed state of the microcheck valve with triple fingers in backward (reverse) flow at a flow rate of 75 μl/min. Compared to the CMP with a single finger, the microstructure was not completely inserted into the entrance of the PDMS microchannel, which might be due to the slightly swollen SU-8 structures during the release process (or misalignment between the microstructure and the PDMS microchannel during the bonding process). However, it should be noted that the fluid was unable to reversely flow through the microchannel due to an increase in the flow resistance under backward flow. Compared to the valves that use single and triple fingers, an increased flow rate (80 μl/min) was needed for the microcheck valve that use a quintuple-finger structure (i.e., five fingers) to push the microstructure (Fig. 5e and f). This might be because the surface area of the CMP gradually increased as the number of fingers increased, which generates a larger friction force, and thus requires more flow rate to actuate the microcheck valve. In addition, as the

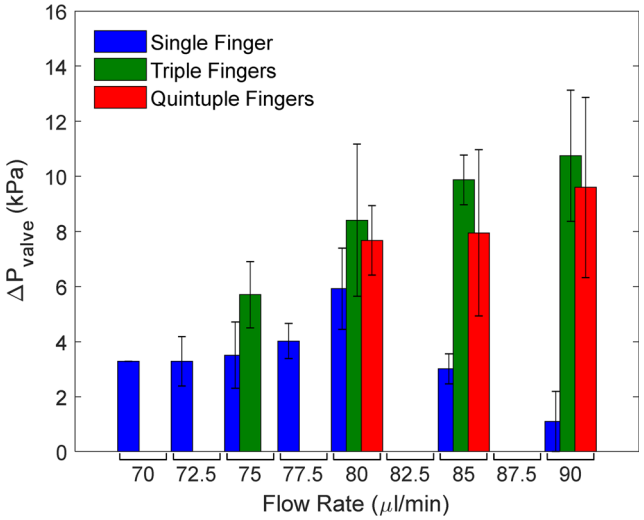

Fig. 6 Difference in the pressure drop (ΔP_{valve}) of microcheck valves between forward and backward flows with respect to low flow rate (low-*Re*) values. 70 μl/min (*Re* = 0.197), 75 μl/min (*Re* = 0.211), and 80 μl/min (*Re* = 0.225) is the minimum flow rate required to actuate (trigger) the single-finger, triple-finger, and quintuple-finger structures during backward flow, respectively

number of fingers increases, the lateral length of microstructure increases. Therefore, the longer microstructure might be slightly tilted during the movement, and require extra hydraulic forces.

To characterize the rectifying performance quantitatively, the pressure drop across the inlet and outlet of the microchannel was experimentally measured for both the open and closed states under various flow rates using a syringe pump and a pressure sensor. Figure 6 shows the measured pressure drops of three different microcheck valves under forward and backward flows in a range of flow rate between 70 μl/min and 90 μl/min. The *Re* was calculated based on following definition (White 2015),

$$Re = \left(\frac{\rho D_H}{\mu A}\right) Q \tag{2}$$

where ρ and D_H are the density of the fluid and hydraulic diameter for a given channel geometry, respectively, μ is the dynamic viscosity of the fluid, and A is the cross-sectional area of the microchannel with 300 μm width and 95 μm height, which calculates the hydraulic diameter of ~144 μm (=4 × cross-sectional area/wetted perimeter). The minimum flow rate for the activation of the valve structures during backward flow was measured to be 70 μl/min (*Re* = 0.197), 75 μl/min (*Re* = 0.211), and 80 μl/min (*Re* = 0.225) for single-finger, triple-finger, and quintuple-finger microstructures, respectively. For the microcheck valve using triple-finger microstructure, the difference in the pressure drop between the backward and forward flows (i.e., ΔP_{valve}) almost linearly increased as *Re* increased, thus demonstrating an efficient fluidic performance to rectify low-*Re* flows. The ΔP_{valve} of the microcheck valve using single-finger microstructure also gradually increased from a flow rate of 70 μl/min to 80 μl/min. However, ΔP_{valve} significantly decreased after a flow rate of 85 μl/min. This might be because the reverse flow was not efficiently blocked by the single-finger microstructure owing to increased leakage flows as the flow rate increased, indicating an optimal operating range of flow rate between 70 μl/min and 80 μl/min for the single-finger microstructure. The ΔP_{valve} of the microcheck valves using triple-finger and quintuple-finger microstructures yielded a higher value compared to that of a single-finger structure for the same *Re*, as shown in Fig. 6. This is because the flow resistance in the backward direction significantly increased compared to the valve that used a single-finger microstructure. As the number of fingers increased, the length of the fluid's streamline also became longer during the backward flow because the physical surfaces where fluid must pass through significantly increased as well. Although the flow resistance in the forward direction simultaneously increased, it was relatively small compared to the increased flow resistance in the backward direction, and thus increased the overall ΔP_{valve}. However, it should be noted that the ΔP_{valve} decreased as the number of fingers increased from three to five at the same flow rate values. This might be because the increase in flow resistance during the forward flow is now comparable to the increase in the flow resistance in the backward direction, which is not negligible anymore. As the number of fingers increases to five, fluid must come in contact with very large surfaces (i.e., vertical SU-8 walls) to escape the chamber even though the valve is in an open state (see Fig. 5e and f). Consequently, the microcheck valve with a quintuple-finger design caused ΔP_{valve} decreases compared to the triple-finger design, thereby implying that the triple-finger microstructure elicited the best device performance (i.e., an average pressure drop difference of 10.75 kPa at an *Re* value of 0.253) to rectify low-*Re* flows in this study.

5 Conclusions

In summary, simple, self-regulating, and reliable microfluidic check valves using comb-shaped moving plug were successfully demonstrated to rectify low-*Re* flows in microchannels. The microfabrication methods, including soft lithography and photolithography using double-layered photoresists films were used to create microchannels and free-moving (suspended) comb-shaped microstructures, respectively. The comb-shaped moving plugs in the microchannel effectively prevented backflow in the closed state to ensure that the microchannel remained completely blocked, but allowed forward flow in the open state. The chronic leakage issue in reverse flow could be improved considerably by the multiple blocking of flows through the comb-shaped moving plug. The number of fingers of the comb-shaped moving plug was also

controlled to investigate the effect of the number of fingers on the rectification performance. As a result, the microfluidic check valve using triple-finger design yielded the highest average pressure drop difference between the backward and forward flows at low-*Re* values measured, thus demonstrating a highly efficient microfluidic rectifier. This study supports the feasibility of the development of efficient, biocompatible, and reliable microvalve systems for various lab-on-a-chip and biomedical applications, such as drug delivery, cell separators, and micropumps.

Acknowledgements This work was supported by the National Research Foundation of Korea (NRF) grant funded by Korean Ministry of Education (Grant No. NRF- 2018R1D1A1B07051411).

References

M.L. Adams, M.L. Johnston, A. Scherer, S.R. Quake, J. Micromech. Microeng. **15**, 1517 (2005)
D.J. Beebe, J.S. Moore, J.M. Bauer, Q. Yu, R.H. Liu, C. Devadoss, B.-H. Jo, Nature **404**, 588 (2000)
D.C.S. Bien, S.J.N. Mitchell, H.S. Gamble, J. Micromech. Microeng. **13**, 557 (2003)
Y. Cheng, X. Ye, Z. Ma, S. Xie, W. Wang, Biomicrofluidics **10**, 014118 (2016)
S. Chung, J.K. Kim, K.C. Wang, D.-C. Han, J.-K. Chang, Biomed. Microdevices **5**, 311 (2003)
A.J. deMello, Nature **442**, 394 (2006)
P. Gravesen, J. Branebjerg, O.S. Jensen, J. Micromech. Microeng. **3**, 168 (1993)
A. Groisman, S.R. Quake, Phys. Rev. Lett. **92**, 094501 (2004)
E.F. Hasselbrink Jr., T.J. Shepodd, J.E. Rehm, Anal. Chem. **74**, 4913 (2002)
C. Henry, J.-P. Minier, G. Lefèvre, Adv. Colloid Interf. Sci. **185–186**, 34 (2012)
J.W. Hong, V. Studer, G. Hang, W.F. Anderson, S.R. Quake, Nat. Biotechnol. **22**, 435 (2004)
M. Hu, H. Du, S.-F. Ling, Y. Fu, Q. Chen, L. Chow, B. Li, J. Micromech. Microeng. **14**, 382 (2004)
S.-B. Huang, Y. Zhao, D. Chen, H.-C. Lee, Y. Luo, T.-K. Chiu, J. Wang, J. Chen, M.-H. Wu, Sens. Actuators B **190**, 928 (2014)
D. Irimia, S.-Y. Liu, W.G. Tharp, A. Samadani, M. Toner, M.C. Poznansky, Lab Chip **6**, 191 (2006)
D. Kim, D.J. Beebe, Sens. Actuators A **136**, 426 (2007)
H. Kim, J. Kim, Microfluid. Nanofluid. **16**, 623 (2014)
B.J. Kirby, T.J. Shepodd, E.F. Hasselbrink Jr., J. Chromatogr. A **979**, 147 (2002)
B.J. Kirby, D.S. Reichmuth, R.F. Renzi, T.J. Shepodd, B.J. Wiedenman, Lab Chip **5**, 184 (2005)
E.T. Lagally, I. Medintz, R.A. Mathies, Anal. Chem. **73**, 565 (2001)
A.C. Lamont, E.C. Reggia, R.D. Sochol, in Proc. *IEEE 30th Int. Conf. Micro Electro Mech. Syst.* (2017), pp. 1304–1307
K.H. Lau, A. Giridhar, S. Harikrishnan, N. Satyanarayana, S.K. Sinha, Microsyst. Technol. **19**, 1863 (2013)
C.-C. Lee, G. Sui, A. Elizarov, C.J. Shu, Y.-S. Shin, A.N. Dooley, J. Huang, A. Daridon, P. Wyatt, D. Stout, H.C. Kolb, O.N. Witte, N. Satyamurthy, J.R. Heath, M.E. Phelps, S.R. Quake, H.-R. Tseng, Science **310**, 1793 (2005)
D.C. Leslie, C.J. Easley, E. Seker, J.M. Karlinsey, M. Utz, M.R. Begley, J.P. Landers, Nat. Phys. **5**, 231 (2009)
J. Loverich, I. Kanno, H. Kotera, Microfluid. Nanofluid. **3**, 427 (2007)
S.S. Massenburg, E. Amstad, D.A. Weitz, Microfluid. Nanofluid. **20**, 94 (2016)
B. Mosadegh, C.-H. Kuo, Y.-C. Tung, Y.-S. Torisawa, T. Bersano-Begey, H. Tavana, S. Takayama, Nat. Phys. **6**, 433 (2010)
N.-T. Nguyen, T.-Q. Truong, Sens. Actuators B **97**, 137 (2004)
N.-T. Nguyen, T.-Q. Truong, K.-K. Wong, S.-S. Ho, C.L.-N. Low, J. Micromech. Microeng. **14**, 69 (2004)
K.W. Oh, C.H. Ahn, J. Micromech. Microeng. **16**, R13 (2006)
K. Ou, J. Jackson, H. Burt, M. Chiao, Lab Chip **12**, 4372 (2012)
D.S. Reichmuth, T.J. Shepodd, B.J. Kirby, Anal. Chem. **76**, 5063 (2004)
R.D. Sochol, M.E. Dueck, S. Li, L.P. Lee, L. Lin, Lab Chip **12**, 5051 (2012a)
R.D. Sochol, S. Li, L.P. Lee, L. Lin, Lab Chip **12**, 4168 (2012b)
R.D. Sochol, C.C. Glick, K.Y. Lee, T. Brubaker, A. Lu, M. Wah, S. Gao, E. Hicks, K.T. Wolf, K. Iwai, L.P. Lee, L. Lin, in Proc. *IEEE 26th Int. Conf. Micro Electro Mech. Syst.* (2013a), pp. 153–156
R.D. Sochol, C.C. Glick, A. Lu, M. Wah, T. Brubaker, K.Y. Lee, K. Iwai, L.P. Lee, L. Lin, in Proc. *17th Int. Conf. Solid-State Sens. Actuators Microsyst.* (2013b), pp. 2201–2204
R.D. Sochol, A. Lu, J. Lei, K. Iwai, L.P. Lee, L. Lin, Lab Chip **14**, 1585 (2014)
T. Thorsen, S.J. Maerkl, S.R. Quake, Science **298**, 580 (2002)
M.A. Unger, H.-P. Chou, T. Thorsen, A. Scherer, S.R. Quake, Science **288**, 113 (2000)
M. Vázquez, B. Paull, Anal. Chim. Acta **668**, 100 (2010)
Y.-C. Wang, M.H. Choi, J. Han, Anal. Chem. **76**, 4426 (2004)
J.A. Weaver, J. Melin, D. Stark, S.R. Quake, M.A. Horowitz, Nat. Phys. **6**, 218 (2010)
F.M. White, Fluid Mechanics, 8th ed. (McGraw-Hill, New York, 2015)
H.M. Wyss, D.L. Blair, J.F. Morris, H.A. Stone, D.A. Weitz, Phys. Rev. E **74**, 061402 (2006)
D. Xu, L. Wang, G. Ding, Y. Zhou, A. Yu, B. Cai, Sens. Actuators A **93**, 87 (2001)
R. Zengerle, J. Ulrich, S. Kluge, M. Richter, A. Richter, Sens. Actuators A **50**, 81 (1995)
X. Zhang, N. Xiang, W. Tang, D. Huang, X. Wang, H. Yi, Z. Ni, Lab Chip **15**, 3473 (2015)
X. Zhang, Z. Zhu, N. Xiang, Z. Ni, Biomicrofluidics **10**, 054123 (2016)